Journal of
Composites Science

MDPI

Article

Effects of Alkaline and Carboxilated Graphene Oxide (CGO) Treatment on Mechanical, Thermal, and Electrical Properties of Jute Fiber-Reinforced Epoxy Composites

Hironmoy Chowdhury [1], Atik Saha [1], Mahbub Hasan [1,*] and Julfikar Haider [2,*]

[1] Department of Materials and Metallurgical Engineering, Bangladesh University of Engineering and Technology, Dhaka 1000, Bangladesh; hironmoy.ch.07@gmail.com (H.C.); atiksaha151@gmail.com (A.S.)
[2] Department of Engineering, Manchester Metropolitan University, Manchester M12 5GN, UK
* Correspondence: mahbubh@mme.buet.ac.bd (M.H.); j.haider@mmu.ac.uk (J.H.)

Abstract: Sustainable and eco-friendly materials are vital for structural and energy storage applications. Synthetic fiber composites have long been utilized, but their high manufacturing cost and negative environmental impacts are concerning. This study aims to enhance the mechanical strength, thermal stability and electrical conductivity of jute fiber–reinforced epoxy composites by hand-lay-up technique with fiber surface modification with alkali (KOH) and carboxilated graphene oxide (CGO). Fourier transform infrared spectroscopy and field emission scanning electron microscopy confirmed fiber surface modification and the presence of CGO particles over the fiber surface. Differential scanning calorimetry was used to analyze the thermal stability and crystallinity of the samples. The electrical conductivity was measured by an electrometer, and the mechanical properties were assessed through tensile and flexural strength tests. Alkaline and CGO-treated jute fiber epoxy composites exhibited remarkable enhancement in mechanical properties, which were attributed to improved fiber-matrix interfacial bonding. Electrical conductivity also improved significantly. However, a trade-off between mechanical and electrical properties, particularly due to the susceptibility of cellulose to alkaline treatment, warrants optimizing the performance of the composites. The developed composites would be suitable for industrial applications where improved mechanical properties, thermal stability, and electrical conductivity are required.

Keywords: natural fiber composite; jute; epoxy; carboxilated graphene oxide (CGO); mechanical properties; electrical conductivity

Academic Editor: Wen-Cheng Chen

Received: 11 January 2025
Revised: 19 February 2025
Accepted: 21 February 2025
Published: 24 February 2025

Citation: Chowdhury, H.; Saha, A.; Hasan, M.; Haider, J. Effects of Alkaline and Carboxilated Graphene Oxide (CGO) Treatment on Mechanical, Thermal, and Electrical Properties of Jute Fiber-Reinforced Epoxy Composites. *J. Compos. Sci.* **2025**, *9*, 104. https://doi.org/10.3390/jcs9030104

1. Introduction

Natural fiber-reinforced polymer composites offer advantages, such as being lightweight, cost-effective, versatile, and environmentally friendly, making them viable alternatives to traditional fillers such as mica, calcium carbonate and glass [1]. The shift toward natural, renewable, and biodegradable materials such as jute is crucial for sustainability amidst increasing synthetic pollution. The ability of natural fiber composites to enhance physical, mechanical, and thermal properties has been studied for various advanced applications. There are many emerging research areas, such as nanomaterials, bioplastic packaging, and 3D printing, that highlight challenges and future directions for commercial success [2]. The amphiphilic nature of graphene enhances interfacial adhesion in natural fiber-reinforced polymer composites. Strategies such as employing graphene-based

materials as hybrid fillers with natural fibers and coating natural fibers with graphene oxide or reduced graphene oxide before adding them to polymer matrices have been developed. These strategies drive innovations in energy storage, drug delivery, biosensors, electronic textiles, medical implants, and ballistic protection armor [3]. However, natural fiber composites suffer from poor mechanical and interfacial properties, and jute fibers can act as a substrate material for depositing graphene layers before embedding in polymer matrix [4].

Ashaduzzaman et al. studied natural fiber composites with desired features for structural applications. Aqueous glycine treatment was applied to untreated and alkali-treated jute yarns, significantly enhancing their chemical, thermal, morphological, and mechanical properties [5]. Compared with the untreated yarns, the alkali-treated jute yarns (ATG) improved the tensile strength and strain properties by approximately 105% and 50%, respectively. These enhancements position glycine-treated jute yarns as promising reinforcements for woven or multi-axial textile composites in structural applications. In the research of Dilfi et al., it was clearly determined that the performance of a composite material depends mainly on the interfacial properties of the reinforcement and the matrix material where the stress transfer from the matrix to the reinforcement occurs through the interface. In addition, the fiber-matrix adhesion plays an important role in the load-transfer ability of the interface. Thus, a good interface with better fiber–matrix adhesion would enhance the mechanical properties of the composite. Hydroxyl-functionalized CNTs were successfully grafted onto ramie fiber surfaces in a KH560 solution, as confirmed by SEM and FTIR analyses. This modification significantly enhanced the flexural, tensile, and interlaminar shear strength (ILSS) properties of the composite plates by improving the fiber–matrix interface. Additionally, the DMA results showed an increased glass transition temperature and reduced damping peaks, further indicating improved interfacial bonding [6]. In another work by Dang et al., the ILSS of the composites was shown to be influenced by the size and content of graphene oxide (GO). Untreated and GO-treated ramie fiber (RF)-reinforced polypropylene (PP) composites were prepared via hot pressing [7]. Roy et al. established that GO was an effective surface modifier, significantly enhancing the interfacial adhesion between RFs and PP in the composites [8]. The effects of low-concentration alkali treatment on jute fibers were studied, revealing significant improvements in mechanical, physical, and thermal properties. Prolonged alkali treatment increased tensile strength by 82% and elongation at break by 45%, primarily due to the removal of non-cellulosic materials. The treatment also reduced fiber hydrophilicity, enhancing fiber-matrix interface bonding. These findings suggest the potential for industrial applications of low-concentration alkali- and GO-treated jute fibers in polymer composite manufacturing. Nayab-Ul-Hossain et al. [9] conducted an experiment on increasing the electrical conductivity of natural fibers. Different chemical treatments have been explored to reduce the surface resistance of jute fibers. The naturally occurring compact structure of jute fibers makes their surface less permeable, which hinders the conductivity of electricity. However, after modification using detergent, sequestering agents, NaOH, and H_2O_2, the surface becomes more porous and less resistant to electricity conduction, which makes the modified jute fibers suitable for use as low- to medium-voltage insulators, as well as conductive materials in applications requiring low current flow.

Some studies have been conducted on treating jute fibers with graphene or graphene oxide to improve their mechanical properties to some extent. However, studies are required to further improve the mechanical and electrical properties of treated jute fiber–reinforced polymer composites. Therefore, the main objective of this research is to explore the changes in the mechanical strength, thermal stability and electrical conductivity of jute fiber epoxy composites utilizing fiber surface modification with an alkali solution and carboxylated graphene oxide (CGO). As several approaches have been used to develop

conductive natural fibers, this work is focused on studying the behavior of chemically treated and conductive nanoparticle-coated jute fiber-reinforced epoxy matrix composites. Hemicellulose, lignin, and pectin are removed from the surface to create better interfacial bonding between the matrix and fibers. Enhancing the surface roughness of fibers is one of the vital objectives of surface treatment [10]. Several surface treatment processes are available [11–14]. Because KOH treatment is inexpensive and cost-effective on a broad scale, it was chosen for the present research.

2. Materials and Methods

2.1. Chemicals and Materials

Untreated dried jute fibers were collected from rural areas of the Rajshahi division of Bangladesh. Potassium hydroxide (KOH) was purchased from Sigma Aldrich, Darmstadt, Germany. The chemicals in the synthesis process were used as received. Epoxy resin (Araldite) and Ethyleneamine hardener (Araldite) were purchased from India. Graphite oxide (GO) was synthesized from graphite powder using a modified Hummer's method. The overall chronology of the oxidation of graphite to produce graphite oxide and finally treatment with chloroacetic acid to develop multilayered CGO, which can improve the potential of graphene oxide, as was found in a previous study [15].

2.2. Fiber Surface Treatment and Composite Fabrication

Initially, untreated jute fibers were collected and treated with hot water at 60 °C for 1.0 h and at 100 °C for 30 min to remove organic contaminants. The fibers were then dried in an oven at 80 °C for 40 min to remove any moisture. Next, 100 mL of KOH solution was prepared at concentrations of 1.0, 4.0, and 6.0 wt.%. Simultaneously, the dried fibers were cut into 20 cm long pieces, dipped into the prepared alkaline solutions for 2 h, and further oven-dried at 80 °C for 40 min. CGO was primarily in water as a solution and was subjected to ultrasonic cleaning in a sonication bath with water as a medium for 30 min to break the agglomerated CGO particles. The jute fibers were dipped for 40 min into 80 mL of CGO solution. Then, the solution with jute fibers inside was heated at 70 °C for 1.0 h to minimize CGO particle loss. Figure 1 presents the key steps during composite fabrication.

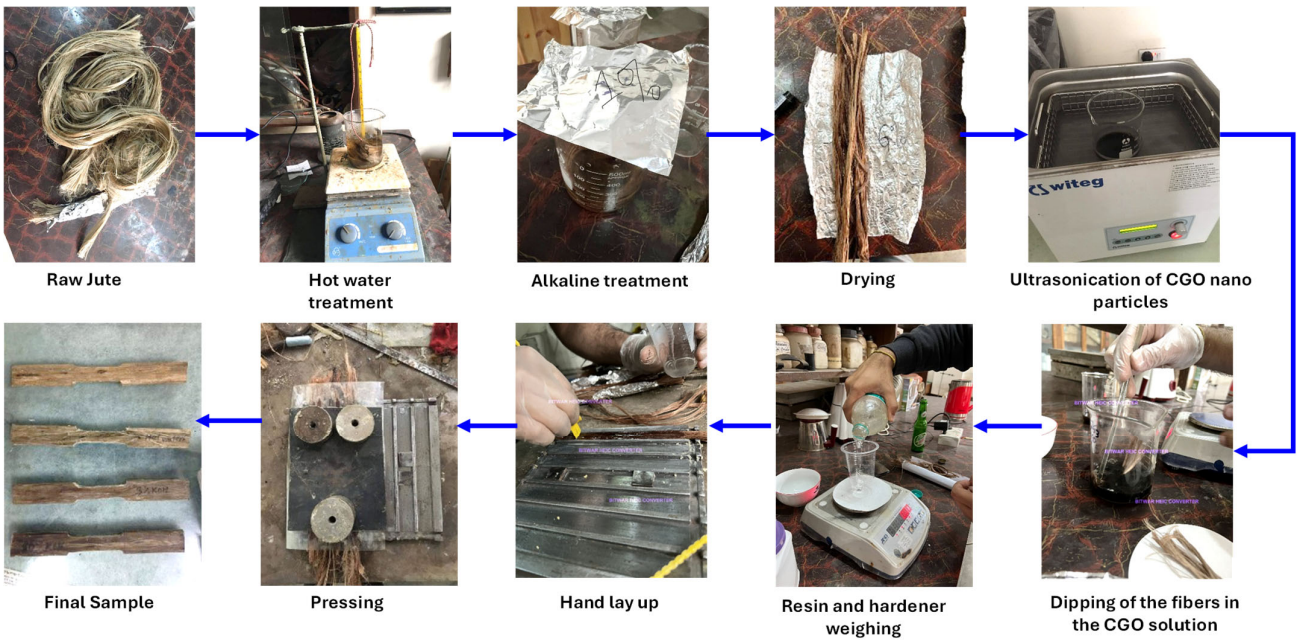

Figure 1. Jute-epoxy composite fabrication process flow.

A mild steel mold was prepared in-house with dimensions of 250 mm × 25 mm × 3.5 mm, and seven distinct vertical grooves with the same width were prepared. Epoxy resin as the matrix material and peroxide as the hardener were blended by manual stirring to dispense the mix in the matrix composite fabrication. The ratio of epoxy to hardener in the mixture was maintained at 10:2. Epoxy resin was poured slowly from the container to prevent any bubble formation, which would increase the porosity of the composite, leading to degradation of the mechanical properties. Then, the mixture was kept inside a refrigerator for 10 min so that the gas bubbles that formed during pouring and mixing could disappear. A release agent (wax) was applied to the surface of the mold to enable easy removal of the prepared composites after curing the mold in open air at room temperature. Each layer of parallel-ply 25 cm long bundle of jute fiber was placed inside the mold gap under the application of tension on two opposite sides. The hand-lay-up technique was adopted to produce composite slabs with 20.0 wt.% of fiber loaded in two layers. The resin material was poured after layer-by-layer mixing. Appropriate impregnation of the resin material and flow was ensured using a roller. Milot paper was placed on top of the casting and pressed with a weight to avoid any adhesion of the epoxy matrix with the roller and the weight body and to obtain a defect-free smooth composite surface.

2.3. Characterization Techniques

2.3.1. Differential Scanning Calorimetry (DSC)

DSC measurements were performed using a thermal analyzer (TA Instrument, Delaware, USA, Model No. Q10). A heating rate of 10 °C/min and a sample weight of 3–4 mg in an aluminum crucible with a pin hole were used in a nitrogen atmosphere (50 mL/min).

2.3.2. Fourier Transform Infrared Spectroscopy (FTIR)

A Bruker alpha T (Germany) spectrometer was used to perform Fourier transform infrared spectroscopy in compliance with ASTM E168-16. After obtaining the necessary powdered sample, it was dissolved in chloroform, and this solution was allowed to evaporate over a KBr salt plate, which was held in place to allow infrared light through a tiny split that showed directionality. The plate absorbs molecular energy when the infrared radiation hits it, producing an interferogram that is then transformed into a spectrum for FTIR analysis, which measures the range of infrared wavelengths that a material absorbs. Each substance within the sample was subjected to infrared (IR) light. In order to determine the molecular composition and structure of individual substances, energy absorption from infrared light at different wavelengths was investigated.

Materials can be quantified using the FTIR material characterization approach as long as a standard curve with known amounts of the component of interest can be constructed. Using FTIR analysis, one can identify unknown components, additives within polymers, and surface contamination on a material. Alkali-treated and untreated natural fibers are subjected to FTIR measurements, which measure the absorbance in the 400–6000 cm^{-1} wavenumber range [16]. The content of natural fibers, including cellulose, hemicellulose, lignin, pectin, and water molecules, is represented by each characteristic peak in the spectra [17].

2.3.3. Scanning Electron Microscopy (SEM)

A high-energy electron beam was used to scan the sample surface to create scanning electron microscope images of the surface. In the present research, a ZEISS Sigma 300 VP scanning electron microscope (Oberkochen, Germany) was used to characterize the top surfaces of the specimens. To view the inherent surface of the fibers, the first specimen consisted of untreated jute fibers. The second specimen was alkali-treated jute fiber, which was examined to view the change in surface morphology due to alkali treatment. Finally,

an alkali+CGO-treated fiber sample was observed via the SEM to determine the effect of CGO particles on the alkali-treated fibers before curing. The specimens were sputter-coated with a thin layer of gold to prevent electrical charging during the examination. An accelerating voltage of 2 kV was used to collect the SEM images.

2.4. Mechanical and Electrical Testing Procedure

2.4.1. Ultimate Tensile Testing

The ASTM D638-10 test protocol was used to measure the tensile characteristics of each prepared sample. The tensile strength of laminated composites was assessed using a universal testing machine (UTM). The tests were repeated on five samples for each type of composite. Each sample had consistent dimensions (length: 250 mm, width: 25 mm, and thickness: 3.5 mm) and was manufactured in compliance with the ASTM standard. They were placed in the grips of an Instron 1195 universal mechanical testing machine (Massachusetts, USA), which can support loads up to 100 kN, and loaded monotonically in tension at a crosshead speed of 2.5 mm/min. The tensile specimens were also gripped by an extensometer to measure the real extension values and to avoid any variation due to an unavoidable slippage of the samples from the grips.

2.4.2. Flexural Test

Three-point bending tests or flexural tests were conducted as per ASTM D790. The dimensions of the specimens were 250 mm in length, 25 mm in width, and 3.5 mm in thickness. The crosshead speed was 5 mm/min, and the span length between the supports was 100 mm for all the samples. The loading nose and supports were positioned to conduct the three-point bending tests. Load deflection data were collected while the load was applied to the specimen at the prescribed crosshead speed. The test was terminated when the outer surface of the test specimen ruptured. The flexural strength was calculated via the following equation.

$$\sigma = \frac{3FL}{2bd^2} \quad (1)$$

where d and b represent the depth and width of the specimen, respectively, L signifies the span length, and F symbolizes the net flexural load applied on the composite specimens.

2.4.3. Electrical Conductivity

A Keithley 6517B electrometer device was used to determine the current flow at 50 volts for five specimens. The specimens were fabricated with dimensions of 25 mm × 20 mm × 2.5 mm for measuring electrical conductivity. An electrometer measures the current (I) at an applied specific voltage. The electrical resistance (R) of the specimens was determined from Equation (2). Finally, the electrical conductivity (σ) can be calculated by Equation (3).

$$R = \frac{V}{I} \quad (2)$$

$$\sigma = \frac{RL}{A} \quad (3)$$

where L is the length of the specimen and A is the area of the specimen.

3. Results and Discussion

3.1. Chemical Analysis

FTIR spectra of the untreated, alkali-treated, and alkali + CGO-treated (Figure 2) jute fiber–reinforced epoxy composites (JFRC) revealed that functional groups and chemical bonds were present in the wavenumber ranging from 4000 cm^{-1} to 500 cm^{-1}. The characteristic features of the spectrum of the jute fiber were its lignin, hemicellulose, and α-cellulose constituents. The 3300 cm^{-1} band, ascribed to H-bonded H–O stretching, exhibited greater absorbance in the case of untreated JFRC than that in the other two types of JFRC because of the presence of lignin and hemicellulose. Saha et al. reported that the reduction in intensity is greater for alkali-steam-treated jute because it disrupts the hydrogen bonds between the O–H groups in cellulose and hemicellulose molecules [13]. This finding was in agreement with the almost constant α-cellulose contents even after mercerization of the jute fibers. The peak at 2900 cm^{-1} could be assigned to C–H stretching in methyl and methylene groups.

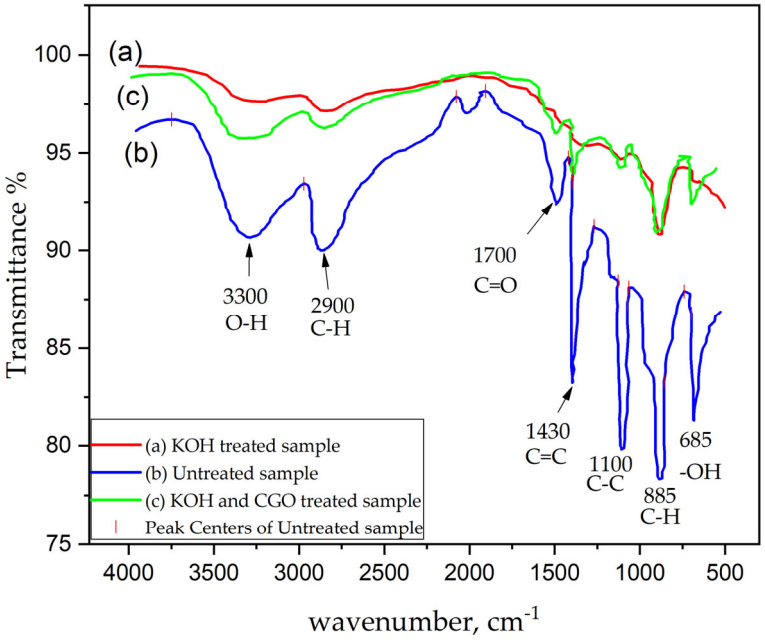

Figure 2. FTIR spectra of 4.0 wt.% KOH treated (line a), untreated (line b) and 4.0 wt.% KOH and CGO treated (line c) JFRCs.

The C=O stretching of carboxylic acid in hemicellulose was represented by the peaks at 1700 cm^{-1} and 1156.60 cm^{-1} [17]. The O-H vibrations of cellulose and hemicelluloses could be linked to the peaks in the frequency range of 1100 cm^{-1} to 1000 cm^{-1}. The C–H bending vibrations of cellulose and lignin were indicated by the peaks in the range of 873.16 cm^{-1} to 728.91 cm^{-1}. The layer between the jute fibers and the epoxy resin in the composite was responsible for the peak between 699.50 cm^{-1} and 598.78 cm^{-1}, which indicated the polymer's skeletal C–N deformation [18]. The peak at approximately 1700 cm^{-1} observed in the spectrum of the untreated fibers disappeared upon alkali treatment. This could be due to the removal of the carboxylic group by alkali treatment through a process called de-esterification. The carboxylic group might also be present in the fiber as traces of fatty acids present in oils. The observed peaks at 1430 cm^{-1} and between 1430 cm^{-1} and 1266 cm^{-1} indicated the presence of lignin and hemicellulose, respectively. The absorbance band at 1430 cm^{-1}, corresponding to the asymmetric deformation of $–CH_3$ groups and the symmetric deformation of C–H bonds in lignin, exhibited a reduced intensity following

the alkali treatment, indicating the removal of lignin. The disappearance of the peak between 1245 and 1259 cm^{-1} after alkalization indicated the complete removal of hemicellulose rather than lignin. This finding implied that hemicelluloses could be more easily removed by alkalization compared to the lignin. The peak observed at 898 cm^{-1} indicated the presence of the $^{N}_{L}$-glycosidic linkages between the monosaccharides. The COOH bending peak was observed between 610–668 cm^{-1}. These results indicated that several chemical reactions took place during the alkalization process of the jute fibers. Owing to their hydrophilic nature, natural fibers are inherently incompatible with the matrix. This compatibility can be improved by applying a hydrophobic coating to the fiber surface. For instance, a CGO coating on jute fiber surfaces has been shown to create a hydrophobic coating, thereby enhancing the fiber–matrix compatibility [6]. The increasing intensity of the –OH and C double bond O peaks of the KOH and CGO treated samples indicated the oxidation of free –OH groups at GO and an increase in the number of –COOH groups on CGO.

It should be noted that, for each sample, the results were obtained separately from the data points. Due to the limited capacity of the relevant software, it was not possible to show all computer-generated curves for all the samples in a single image. Moreover, there were extra noise-like peaks with the values, which made it even more challenging to decipher. Therefore, a compiled graph for the samples was generated without the noise peaks to compare the results easily. The peak points of each curve were also clearly marked. For further clarification, the original FTIR graphs are provided in the Appendix A.

3.2. Thermal Analysis

The thermal behavior of the treated and untreated fiber-reinforced polymer composites (JFRC) is displayed in Figure 3. The individual thermal deterioration characteristics of the matrix and the fibers were combined to create the overall thermal degradation pattern of epoxy resin matrix composites reinforced with untreated, alkali-, and alkali+CGO-treated jute fibers [19]. The DSC curve of the composite reinforced with untreated jute fibers showed that the transition temperature (Tg) to a soften glassy phase occurred at 53 °C, and that a modest endothermic moisture desorption peak was found. The Tg peak moved to a temperature higher than 53 °C for the untreated fiber-reinforced composite, and to 58 °C for the composite reinforced with alkali-treated jute fibers. Finally, the Tg peak moved to an even higher temperature of 64 °C for the CGO and alkali-treated jute fiber reinforced composites. The improved interfacial bonding restricted the mobility of the polymer chains near the fiber–matrix interface, resulting in a higher Tg. This could lead to a decrease in the available surface area needed for moisture desorption through a decrease in moisture evaporation [20]. In a work by Dilfi et al., the increase in the Tg was associated with the decreased mobility of the matrix chains, which was an indication of improved interfacial adhesion between the fiber and the matrix [6].

A broad exothermic peak was observed at 337 °C for the untreated jute–epoxy composite. The area under the curve for the crystalline temperature (Tc) shows how much heat energy is required for hemicellulose degradation. After alkaline treatment, the Tc was approximately 330 °C and the area of the hump decreased due to the removal of non-cellulosic materials such as hemicellulose. However, a reduction in the area under the curve and the Tc found for the CGO-coated fiber–epoxy composite indicated a reduction in the crystalline behavior, which enhanced thermal stability and energy absorption capacity, possibly due to strong interactions between the CGO coating and the polymer matrix. Furthermore, CGO introduced functional groups, such as -COOH and -OH, which helped in improving its compatibility with the polymer matrix. By limiting polymer chain mobility and enhancing heat stability, CGO functioned as an effective reinforcing

nanomaterial. Additionally, CGO suppressed the melting behavior by interfering with the ordered arrangement of the polymer chains.

The sharp endothermic peak appeared at 360 °C for the untreated jute epoxy composite could be due to the degradation of the hemicelluloses and cellulose, respectively, in the fiber part of the composite [21]. The improved wetting of the finely separated fibers by the resins may be the cause of the propensity of the treated composite to release moisture at a higher temperature. From 360 °C for the untreated fiber-reinforced composite to 368 °C for the 4.0 wt.% alkali-treated jute epoxy composite, the cellulose degradation temperature in the fibers of the composites increased. However, the degradation temperature of the alkali+CGO treated was higher than that of the samples treated with 2 °C alkali-treated JFRC.

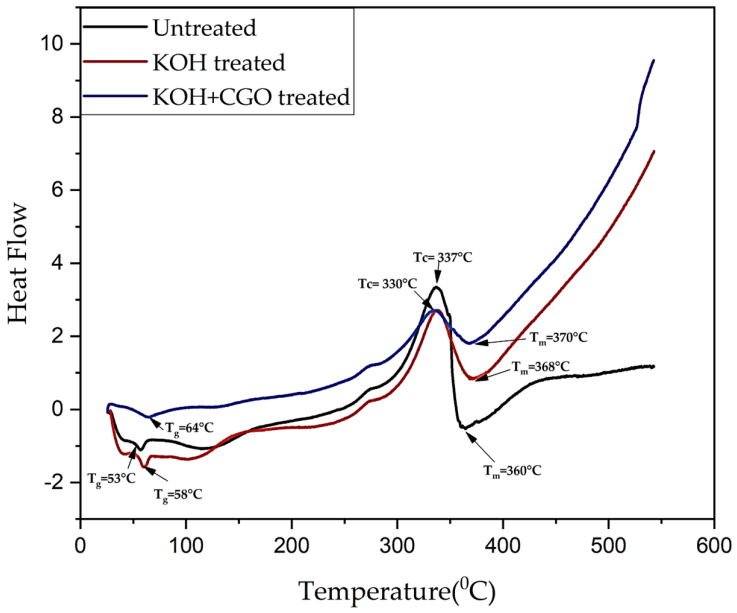

Figure 3. DSC curves of untreated (spectra a), 4.0 wt.% KOH treated (spectra b) and 4.0 wt.% KOH and CGO treated (spectra c) jute fiber–reinforced epoxy composites (JREECs).

The primary breakdown temperatures of the composite resin components remained essentially unchanged. The firmly packed cellulose chain in the alkali-treated fiber composite resisted thermal breakdown in conjunction with the resin, as indicated by the higher degradation temperature of the cellulose in the treated jute composites than in the untreated jute composites. This demonstrated the improved thermal stability of the alkali-treated jute composites [22]. Alkaline treatment removed the non-cellulosic contents of the fibers, which created better adhesion between the fibers and the matrix. The incorporation of CGO nanofillers into the fibers after alkaline treatment reinforced the structure, resulting in better thermal stability than that of the untreated and alkaline-treated fiber composites.

3.3. Morphological Analysis

The surface morphologies of the untreated, alkali-treated, and alkali+CGO-treated jute fibers analyzed by the SEM are shown in Figure 4. The surfaces of the untreated jute fibers (Figure 4a) were smooth and multicellular in nature, whereas rough surface morphology and fragments on the surface of the alkali-treated jute fibers were observed (Figure 4b). This could be because of the removal of the cementing layer, which is composed of waxes, fats, lignin, pectin, and hemicelluloses [23]. Generally, a grooved appearance

with micro-voids was visible after alkali treatment [24]. The CGO-dipped fibers showed a layer-like appearance (Figure 4c). A more uniform and evenly coated fiber surface with only a few flakes was present on the surface, which could be due to good adhesion and interlocking of the CGO particles on the fiber surface grooves [9].

(**a**) (**b**) (**c**)

Figure 4. SEM images of (**a**) untreated, (**b**) 4 wt% KOH treated and (**c**) 4 wt% KOH and CGO-treated jute fiber surfaces.

3.4. Tensile Strength of the Composites

The tensile strength (UTS) of the samples is plotted against different types of JFRCs. Jute fibers were treated with 1.0 wt.%, 4.0 wt.%, 6.0 wt.%, and 8.0 wt.% KOH solutions, and the tensile strengths were compared to those of the untreated, hot water treated, and pure epoxy samples. Figure 5a shows that the untreated JFRC has the lowest UTS of 12.7 MPa. Compared with the untreated JFRC, the hot water-treated JFRC exhibited a significantly greater UTS of 48.1 MPa, which was an increase of 280%. The UTS of the 1% KOH-treated composite further increased to 55.7 MPa, which is an increase of 13.6% compared to that of the hot water-treated JFRC. The 4% KOH-treated composite has a UTS of 67.5 MPa, which is 21% greater than that of the 1% KOH-treated FRC. For alkali-treated JFRCs, the UTS generally increased as the concentration of KOH increased from 1.0 to 4.0 wt.%. Alkaline treatment removes pectin, lignin, and hemicellulose layers from the surface of jute fibers, which increased fiber surface roughness and results in an increase in the UTS of JFRCs due to improved interlocking of the matrix and reinforcement fibers. Additionally, alkali treatment can cause jute fibers to swell and increase in diameter. The expansion of the fiber diameter leads to a larger cross-sectional area, which directly influences the UTS [25]. However, the 6% KOH-treated composite exhibited a lower UTS of 43.8 MPa, which was 35% lower than that of the 4% KOH-treated composite. Among the composites, the 8% KOH-treated composite had the lowest UTS of 28.2 MPa, which was 35% lower than that of the 6% KOH-treated composite. The chemical degradation of jute fibers caused by higher concentrations of alkali can lead to a decrease in the UTS of the JFRC [26,27]. The ability of JFRC to withstand applied forces and resist breaking is compromised due to the breakdown of its internal structure and the weakening of its cellulosic chains.

Therefore, 1.0 wt.% and 4.0 wt.% KOH-treated jute fibers were further treated with a CGO layer to assess its compound effect on the composite properties. Figure 5b clearly shows that the UTS of the 1.0% KOH+CGO-treated JFRC was 35.65% greater than that of the 1% KOH-treated JFRC. The UTS also increased for the 4% KOH+CGO-treated FRC by 18.52% compared to that for the 4% KOH-treated JFRC. In a recent study [27], UTS increased after fiber surface modification by incorporating graphene oxide nanoparticles. The tensile strength increased from 31.9 MPa in the bamboo fiber–reinforced polypropylene (PP) composite to 35.9 MPa in the 0.1GO treated composite (a 12.6% increase). Comparatively, the present research revealed better results for alkali-treated and CGO-

incorporated JFRC. This may occur because of the different matrix materials, the greater availability of hydrogen bonds as functional groups (-OH, -COOH) on the jute fiber surface, and the strong adhesion of the CGO particles to the jute fiber surface. In another study [28], graphene oxide incorporation on the jute fiber surface of JFRC enhanced the tensile strength by approximately 110% compared to that of untreated jute fiber composites by arranging fibers in a parallel direction through individualization. In the present research, a 431.5% increase in tensile strength was obtained after alkali+CGO treatment. The increase in the tensile strength of CGO-treated FRC occurred because alkali-treated jute fibers were coated with CGO particles, which enhanced the interfacial bond strength [4]. The presence of oxygen-containing functional groups in CGO facilitates connections between the cellulosic fibers and the matrix through the formation of chemical bonds. These bonds establish molecular continuity across the composite interface, thereby increasing the tensile properties [29].

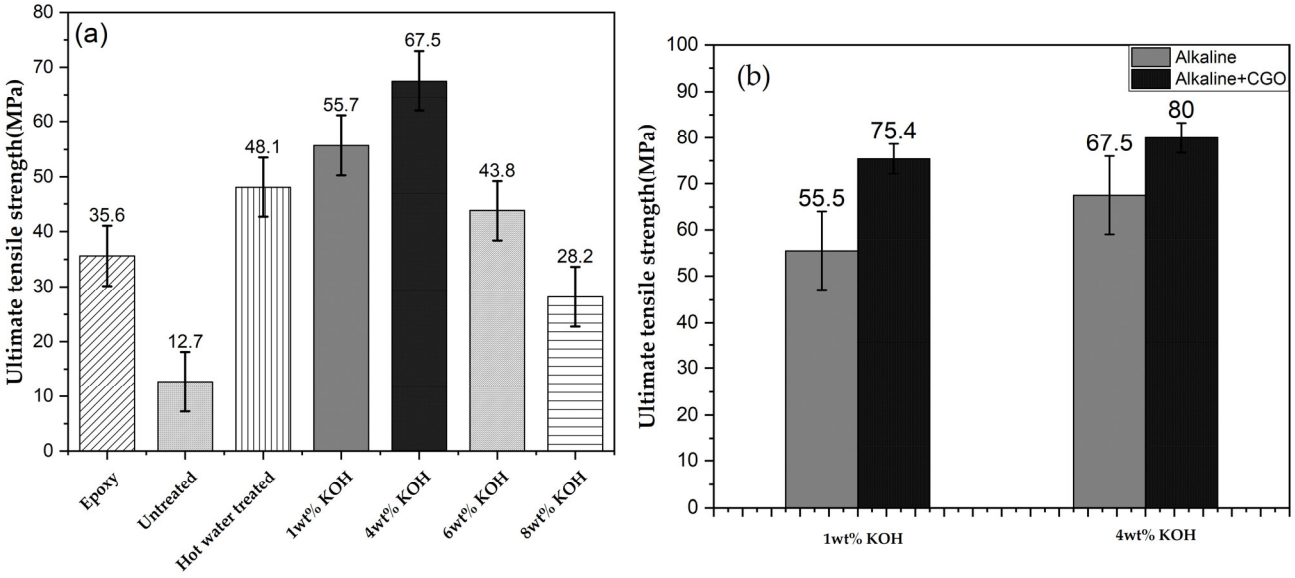

Figure 5. Tensile strength of jute fiber–reinforced epoxy composites with (**a**) various surface treatments and (**b**) 1.0 wt.% and 4.0 wt.% KOH treated JFRC after CGO addition.

3.5. Flexural Strength of the Composites

Figure 6a shows that the untreated JFRC had the lowest flexural strength of 18 MPa, and the 4% KOH-treated FRC had the highest flexural strength of 87 MPa. The 1% KOH-treated FRC is ranked 2nd, and the 6% KOH-treated FRC is ranked 3rd among all the FRCs. Therefore, when the matrix epoxy was reinforced with 1% KOH-treated fibers, the flexural strength increased by 28.8%. The flexural strength increased by 37.4% for the 3% KOH-treated FRC and 49.98% for the 4% KOH-treated FRC. As the alkaline concentration increased from 1% to 4%, the flexural strength increased gradually. An increase in the KOH concentration during the treatment removed the hemicellulose layer from the fiber, which led to an increase in the wettability and, hence, an increase in the flexural strength [28]. However, for alkaline concentrations greater than 4%, the flexural strength gradually decreased. The bar chart (Figure 6a) shows that the flexural strength of the 6% KOH-treated FRC was lower than that of any other alkali-treated JFRC. A decrease in the flexural strength occurs due to the treatment of the fibers with KOH at a relatively high concentration, which might cause the polymer chains to break down, leading to chemical degradation of the jute fibers. This degradation weakens the structural integrity of the material, resulting in a decrease in the flexural strength.

Figure 6b clearly shows that the flexural strength of the 1.0 wt.% KOH+CGO-treated JFRC was 2.7% greater than that of the 1.0 wt.% KOH-treated JFRC. The flexural strength was also 2.3% greater for the 4% KOH+CGO-treated FRC than for the 4% KOH-treated FRC. The slight increase in the flexural strength of the CGO-treated FRC occurred because alkali-treated jute fibers were coated with CGO particles, which enhanced the interfacial shear strength to a small extent [30,31]. A recent study revealed that the flexural strength increased from 42.9 MPa in the untreated bamboo fiber–reinforced PP composite to 53.1 MPa in the 0.1 GO treated composite (a 23.7% increase) [30]. Thus, the flexural strength follows the same trend as the tensile strength. Fiber surface modification and graphene derivative incorporation improve the flexural strength, as achieved in the present research by incorporating another graphene derivative [9].

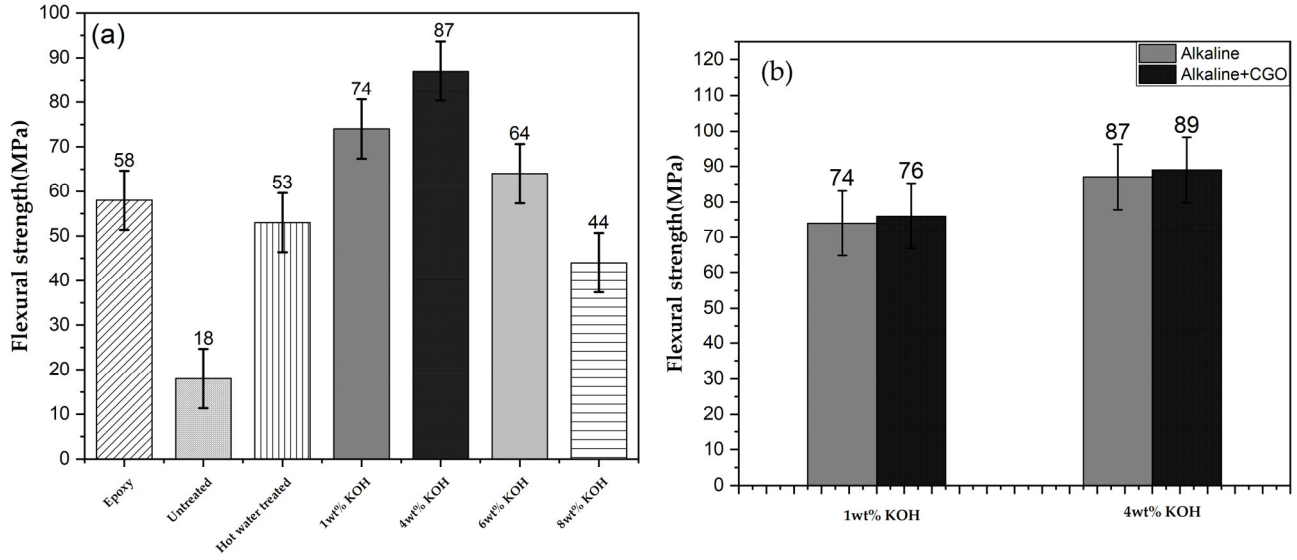

Figure 6. Flexural strength of (**a**) jute fiber–reinforced epoxy composites subject to various surface treatments and (**b**) 1.0 wt.% and 4.0 wt.% KOH treated JFRC after CGO addition.

3.6. Electrical Conductivity of the Composites

Figure 7 shows the electrical conductivity (mS/m) versus chemical surface-treated fiber epoxy composite for all specimens (untreated JFRC, 1.0 wt.% KOH-treated JFRC, 1.0 wt.% KOH+CGO-treated JFRC, 4.0 wt.% KOH, and 4.0 wt.% KOH+CGO-treated JFRC). The results revealed that the 4.0 wt.% KOH+CGO-treated JFRC had the highest electrical conductivity of 2.17×10^{-2} (mS/m), while the untreated JFRC had the lowest electrical conductivity of 4.5×10^{-4} (mS/m). The electrical conductivity of the JFRC increased significantly by approximately 123% after 4.0 wt.% alkali treatment. Further coating with CGO resulted in an increase of approximately 2070% because the electrical conductivity of CGO is very high. Figure 7 also shows that the electrical conductivity of the 4% KOH-treated JFRCs coated with CGO was greater than that of the 1% KOH-treated JFRCs coated with CGO because a high concentration of alkaline solution removes non-cellulosic nonconductive materials (lignin and hemicellulose) on a large scale [9]. This confirms the high electron flow. In addition, the highly electrically conductive CGO layer on the chemically treated surface confirmed that a high electron flow of lignin was present in the untreated jute before chemical processing.

The elasticity and porosity of jute fibers are both impacted by lignin. The lignin that was present in the jute fiber was eliminated when it was altered chemically. The jute fibers gained flexibility and greater porosity after the lignin was removed, which ultimately facilitated more electron passes through the fibers. Therefore, the electrical conductivity of

modified jute fibers increased [23]. When CGO is incorporated into the jute fiber matrix, it forms a conductive network within the composite material. This interconnected network of carbon-based structures provides pathways for the flow of electrons, enhancing the overall electrical conductivity. As the current flow increases for a fixed voltage according to the trend of the bar chart, the conductivity of the composite was calculated using the formula $\sigma = L/RA$ [32]. In a recent study, the electrical conductivity of the untreated fibers increased by 87% due to the fiber surface modification technique, and our work resulted in a more than 4000% increase in the conductivity of the composite because of graphene derivative incorporation [9]. Other data obtained during the conductivity tests are presented in Table 1.

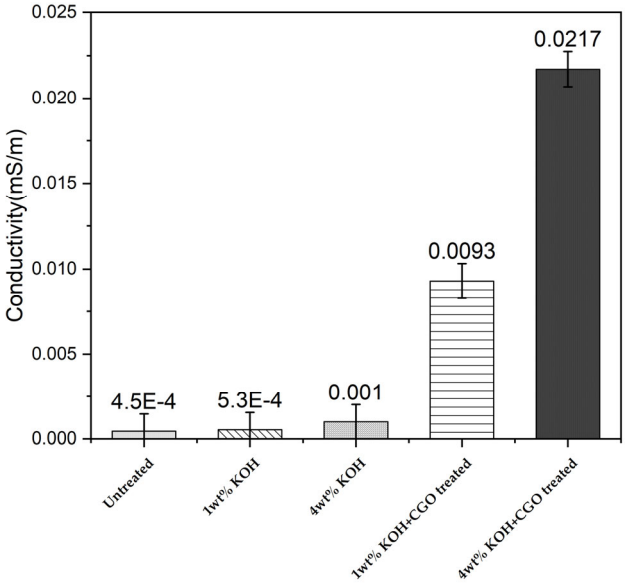

Figure 7. Changes in electrical conductivity of JFRC depending on jute fiber surface modification.

Table 1. Results associated with electrical conductivity measurements.

Composite	Voltage (V)	Current Flow (nA)	Resistance (GΩ)	Specific Resistance (kΩm)	Conductivity (mS)m^{-1}
Untreated	50 V	44.93	1.11	2225.78	4.5×10^{-4}
1%KOH		53.85	0.93	1875.15	5.3×10^{-4}
4%KOH		96.36	0.52	1037.74	1×10^{-3}
1%KOH+CGO		926.00	0.05	107.99	9.3×10^{-3}
4%KOH+CGO		2174	0.02	45.99	2.17×10^{-2}

3.7. Discussion

The degree of adhesion between the fiber and the polymer matrix is the most crucial element in achieving excellent fiber reinforcement in the composite [33]. The polarity and structure of these materials determine the degree of adhesion [34]. The rapid moisture regain caused by the presence of hydroxyl and other polar groups in jute constituents results in weak interfacial interactions between the fibers and the more hydrophobic matrices and poor wettability with the matrix used in this study [35]. Consequently, hydrophobicity must be added to the fibers through appropriate chemical treatments in order to develop composites with better mechanical qualities [36]. In order to reduce moisture absorption, eliminating the hydrophilic elements of jute would strengthen the interfacial link and make the fibers more wettable by the polymer matrix. For composites to have

improved mechanical qualities, both elements are essential. In general, when contrasting the transmittance percentage of the alkali-treated and untreated jute fibers, it was observed that some of the characteristic peaks, which were seen in the spectrum of the untreated fibers, disappeared in the alkali-treated fibers [10]. This could be attributed to the removal of cementing substances such as hemicellulose, lignin, pectin and moisture from the jute fibers [18].

As Figure 6b clearly shows, with the CGO coating on 1.0 wt.% and 4.0 wt.% KOH-treated jute fiber reinforced composites, the difference in flexural strength compared with the flexural strength with only KOH treatment was insignificant. This indicated that the CGO coating did not improve the flexural strength to the same degree as found in the case of tensile strength. As mentioned earlier, CGO coating on the alkali-treated fibers was conducted manually through the dipping process, which might produce non-uniform coating (visible in the KOH+CGO-treated fibers in Figure 4c). Even though ultrasonication was used to ensure uniform dispersion of the CGO particles in the overall solution, precipitation, agglomeration, or poor dispersion of the particles might have occurred [4]. This could cause some inconsistent bonding at the fiber–matrix interface, meaning that the benefit of the CGO coating was not fully realized during the flexural strength testing, in which failure might occur due to a complex combination of shear, compression, and tensile forces.

Table 2 presents a comparison of mechanical strength of the composites prepared with natural fibers treated with carbon-based nanoparticles. The current composite prepared with 4.0 wt.% KOH-treated and CGO-coated jute fibers produced better mechanical strength than the other composites reported in the literature.

Table 2. Comparison of mechanical properties of the best composite in this work with those reported in the literature.

Reference	Material Composition	Fiber Surface Treatment	Nanoparticle Additives	Tensile Strength (MPa)	Flexural Strength (MPa)
Pa and M, 2019 [37]	Jute/Epoxy	Acetone	Graphene Oxide (GO)	28.26	55.41
Sadangi et al. 2021 [38]	Jute/Epoxy	Not mentioned	Graphene Oxide (GO)/Functionalized graphene	58/59	18/18.8
Dilfi et al., 2019 [6]	ramie/epoxy composites	Silane	CNT (Carbon Nano tube)	77	84
Wang et al., 2020 [27]	bamboo-fiber-reinforced polypropylene composites	NaOH	Graphene Oxide (GO)	36	53
Present work	***Jute Fiber/Epoxy Composite***	***KOH (4.0 wt.%)***	***Carboxylated Graphene Oxide (CGO)***	***80***	***89***

The composite materials used in conductive applications should have electrical conductivities of 12^{-10} to 10^{-8} S/cm for Electro Static Discharge, 10^{-8} to 10^{-2} S/cm for moderate conductivity, and above 10^{-2} S/cm for shielding [39]. The best-case scenario obtained for the 4 wt% KOH and CGO-treated jute fiber–epoxy composite showed a conductivity of 2.17×10^{-2} (mS)m^{-1}. Therefore, the fabricated composite could be a feasible option for conductive applications even with a small amount of conductive filler. Generally, non-conductive composites are made conductive by introducing highly conductive nanoparticles, such as CNT and rGO. Here, a range of conductivity was gained by depositing a coating of conductive nanoparticles. At the same time, the incorporation of a small amount of CGO nanoparticles improved mechanical properties of the composites. The unidirectional

fiber pattern helped the nanoparticles create a conductive network within the composites. These composites offer a range of electrical conductivities suitable for various applications, from electrostatic discharge to shielding, while also enhancing mechanical strength, thereby reducing the reliance on additional fillers and improving cost-effectiveness. Additionally, the development of electrically conductive yarns coated with graphene nanoparticles (GNPs) provides opportunities for adaptable and wearable devices, facilitating applications such as human motion detection, soft robotics, and human–machine interfaces [40].

Again, the SEM images of both raw and alkalized surfaces shown in Figure 4 revealed that the raw jute fiber surfaces were smooth, whereas rough surface morphology and fragments on the surface of the alkalized jute fibers were observed. Similar findings were also reported in another work [21]. It was also found that the fiber roughness increased as the treatment time was increased. The rough surface morphology was typical for the treated fibers because of the removal of lignin and hemicelluloses and other structural effects. Here, the concentration of the alkaline solution was varied instead of time. Ultimately, it was evident that both approaches resulted in similar outputs. Thus, alkali treatment resulted in significant change of morphology of the fiber surface and is effective for available contact between the fiber and polymer matrix.

4. Conclusions

An experimental study of alkali-treated and CGO nanoparticle-incorporated jute fiber–reinforced epoxy composite specimens revealed valuable insights into their functional properties and structural characteristics. The mechanical properties gradually improved with up to 4 wt.% KOH treatment because of the removal of non-cellulosic components, which enhanced fiber–matrix interlocking and promoted better adhesion. The increased thermal stability of the alkali-treated composites is attributed to the removal of non-cellulosic materials and improved interfacial interactions. The morphological evidence supported the surface modifications induced by alkali treatment and the CGO coating, further validating the improved adhesion and interlocking between the fibers and the epoxy matrix, and ultimately leading to even better thermal stability and mechanical properties. Although increasing the concentration of alkaline solution may increase the electrical conductivity, the mechanical properties degrade due to structural weakening of the fibers. Therefore, to achieve a balance of high electrical conductivity without compromising the mechanical and thermal integrity, a combination of 4 wt.% KOH treatment and CGO coating could be considered due to their synergistic effects. These findings have important implications for the development of eco-friendly and high-performance composite materials for various engineering applications.

Further optimization and exploration of these treatments could lead to even more enhanced properties and broader applications of these composites. Other tests, such as fracture toughness, wettability and water sorption, can be conducted to understand the beneficial characteristics of the developed composites and customize them for any specific application. In the future, comprehensive studies and investigations on the interfacial chemistry of the matrix, CGO, and cellulose and its effects on the physical, mechanical, and electrical properties may improve the gaps in the current findings.

Author Contributions: Conceptualization, H.C. and A.S.; methodology, H.C., A.S. and M.H.; investigation, H.C. and A.S.; resources, M.H.; data curation, H.C. and A.S.; writing—original draft preparation, H.C. and A.S.; writing—review and editing, M.H. and J.H.; visualization, H.C. and J.H.; validation, M.H. and J.H.; formal analysis, H.C., A.S., M.H. and J.H. All authors have read and agreed to the published version of the manuscript.

Funding: This research received no external funding.

Institutional Review Board Statement: Not applicable.

Informed Consent Statement: Not applicable.

Data Availability Statement: The data presented in this study are available within the article.

Acknowledgments: The authors acknowledge the technical support from the Manchester Metropolitan University, UK and Bangladesh University of Engineering and Technology, Dhaka, Bangladesh.

Conflicts of Interest: The authors declare no conflict of interest.

Appendix A

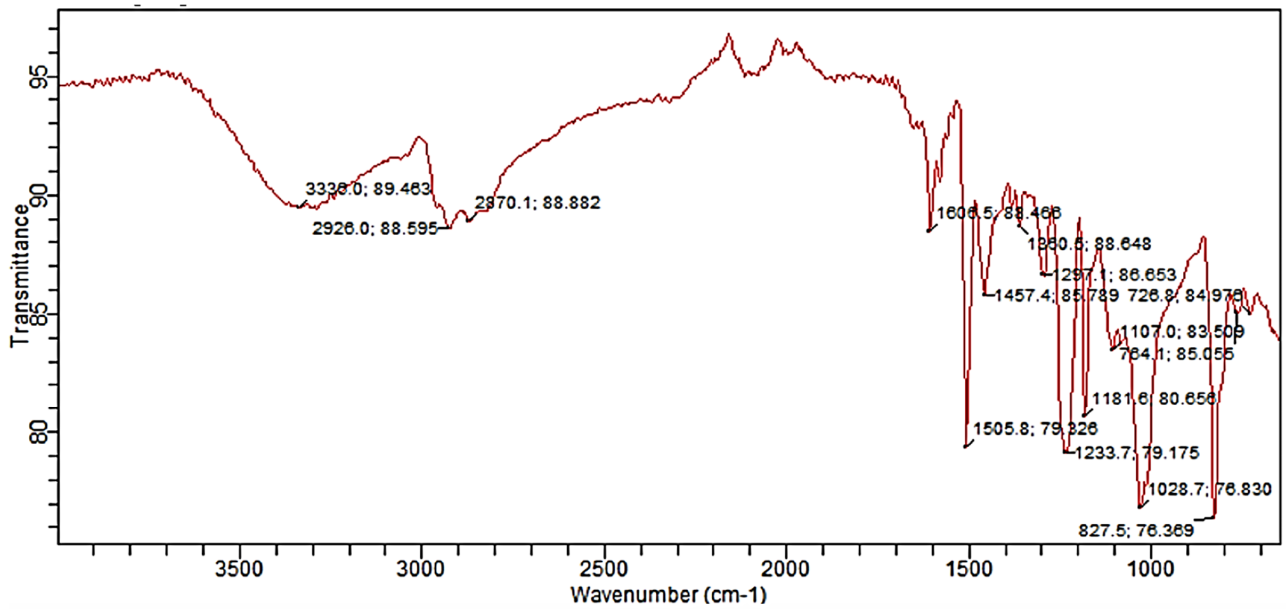

Figure A1. FTIR spectra of untreated jute fiber–reinforced epoxy composite.

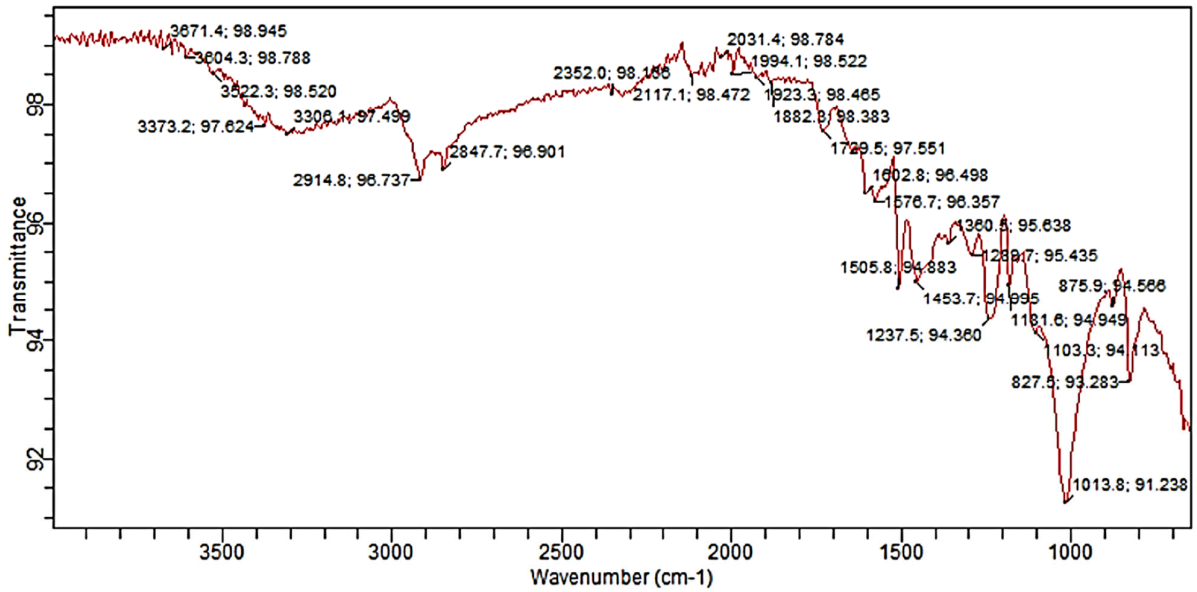

Figure A2. FTIR spectra of 4.0 wt.% KOH treated jute fiber– reinforced epoxy composite.

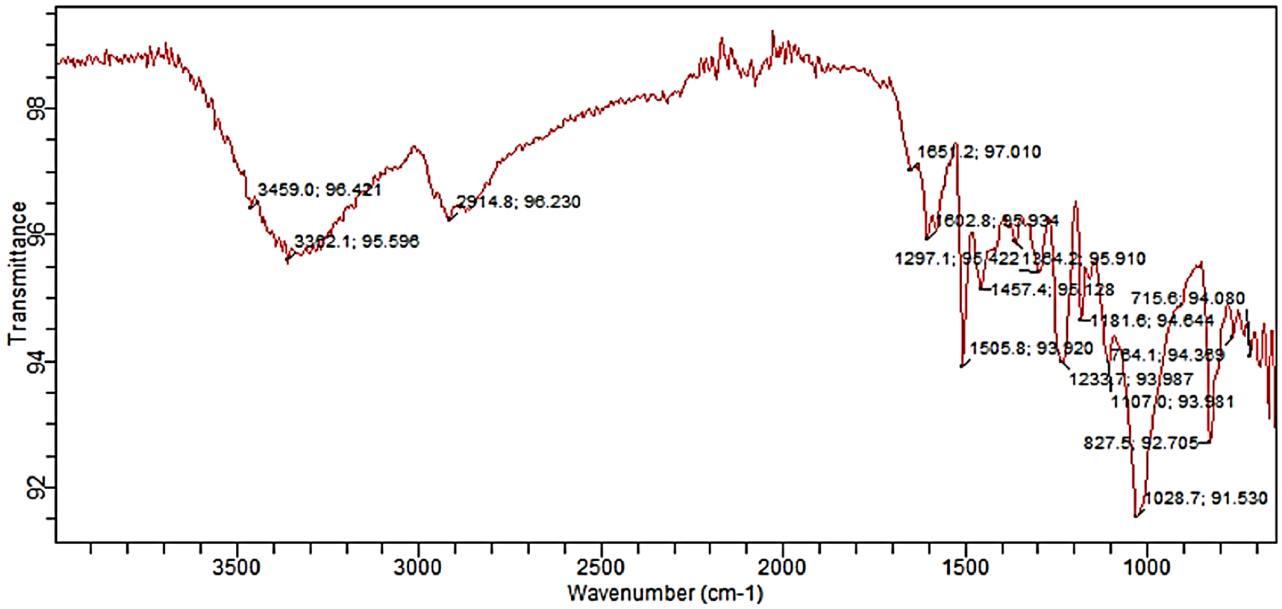

Figure A3. FTIR spectra of 4.0 wt.% KOH and CGO treated jute fiber–reinforced epoxy composite.

References

1. Saba, N.; Jawaid, M. *Epoxy Resin Based Hybrid Polymer Composites*; Elsevier Ltd.: Amsterdam, The Netherlands, 2017. https://doi.org/10.1016/B978-0-08-100787-7.00003-2.
2. Shahinur, S.; Sayeed, M.M.A.; Hasan, M.; Sayem, A.S.M.; Haider, J.; Ura, S. Current Development and Future Perspective on Natural Jute Fibers and Their Biocomposites. *Polymers* **2022**, *14*, 1445. https://doi.org/10.3390/polym14071445.
3. Luz, F.S.; Garcia Filho, F.C.; Del-Rio, M.T.C.; Nascimento, L.F.C.; Pinehro, W.A.; Monteiro, S.N. Graphene-incorporated natural fiber polymer composites: A first overview. *Polymers* **2020**, *12*, 1601. https://doi.org/10.3390/polym12071601.
4. Islam, M.H.; Islam, R.; Dulal, M.; Afroj, S.; Karim, N. The effect of surface treatments and graphene-based modifications on mechanical properties of natural jute fiber composites: A review. *iScience* **2022**, *25*, 103597. https://doi.org/10.1016/j.isci.2021.103597.
5. Ashadujjaman; Saifullah, A.; Shah, D.U.; Zhang, M.; Akonda, M.; Karim, N.; Sarker, F. Enhancing the mechanical properties of natural jute yarn suitable for structural applications. *Mater. Res. Express* **2021**, *8*, 055503. https://doi.org/10.1088/2053-1591/abfd5e.
6. Anna Dilfi, K.F.; Che, Z.; Xian, G. Grafting ramie fiber with carbon nanotube and its effect on the mechanical and interfacial properties of ramie/epoxy composites. *J. Nat. Fibers* **2019**, *16*, 388–403. https://doi.org/10.1080/15440478.2017.1423259.
7. Dang, C.-Y.; Shen, X.-J.; Nie, H.-J.; Yang, S.; Shen, J.-X.; Yang, X.-H.; Fu, S.-Y. Enhanced interlaminar shear strength of ramie fiber/polypropylene composites by optimal combination of graphene oxide size and content. *Compos. Part B Eng.* **2019**, *168*, 488–495. https://doi.org/10.1016/j.compositesb.2019.03.080.
8. Roy, A.; Chakraborty, S.; Kundu, S.P.; Basak, R.K.; Majumder, S.B.; Adhikari, B. Improvement in mechanical properties of jute fibres through mild alkali treatment as demonstrated by utilisation of the Weibull distribution model. *Bioresour. Technol.* **2012**, *107*, 222–228. https://doi.org/10.1016/j.biortech.2011.11.073.
9. Nayab-Ul-Hossain, A.; Sela, S.K.; Hassan, M.N.; Sarkar, A. Surface modification of ligno-cellulosic fiber(jute) to increase electrical conductivity. *Mater. Lett. X* **2020**, *5*, 100036. https://doi.org/10.1016/j.mlblux.2019.100036.
10. Mohanty, A.; A Khan, M.; Hinrichsen, G. Surface modification of jute and its influence on performance of biodegradable jute-fabric/Biopol composites. *Compos. Sci. Technol.* **2000**, *60*, 1115–1124. https://doi.org/10.1016/s0266-3538(00)00012-9.
11. Venkateshwaran, N.; Perumal, A.E.; Arunsundaranayagam, D. Fiber surface treatment and its effect on mechanical and visco-elastic behaviour of banana/epoxy composite. *Mater. Des.* **2013**, *47*, 151–159. https://doi.org/10.1016/j.matdes.2012.12.001.
12. Ali, M.E.; Sultana, Z.; Uddin, M.S.; Mamun, S.A.; Haque, M.M.; Hasan, M. Effect of hydrazine post-treatment on natural fibre reinforced polymer composites. *Mater. Res. Innov.* **2013**, *17 (*Suppl. 2), s19–s26. https://doi.org/10.1179/1432891713z.000000000295.
13. Saha, P.; Manna, S.; Chowdhury, S.R.; Sen, R.; Roy, D.; Adhikari, B. Enhancement of tensile strength of lignocellulosic jute fibers by alkali-steam treatment. *Bioresour. Technol.* **2010**, *101*, 3182–3187. https://doi.org/10.1016/j.biortech.2009.12.010.

14. Ali, M.E.; Sultana, Z.; Uddin, M.S.; Al Mamun, M.S.; Haque, M.M.; Hasan, M. Effect of chemical treatment on palm fibre reinforced polypropylene composites. *Int. J. Mater. Prod. Technol.* **2014**, *48*, 3–17.
15. Hossain, S.; Rahman, S.; Dhar, L.; Quraishi, S.B.; Abser, N.; Rahman, F.; Rahman, M.T. Increasing the potentiality of graphene oxide by chloroacetic acid for the adsorption of lead with molecular dynamic interpretation. *Curr. Res. Green Sustain. Chem.* **2021**, *4*, 100095. https://doi.org/10.1016/j.crgsc.2021.100095.
16. Burrola-Núñez, H.; Herrera-Franco, P.J.; E Rodríguez-Félix, D.; Soto-Valdez, H.; Madera-Santana, T.J. Surface modification and performance of jute fibers as reinforcement on polymer matrix: An overview. *J. Nat. Fibers* **2019**, *16*, 944–960. https://doi.org/10.1080/15440478.2018.1441093.
17. Galletti, A.M.R.; D'alessio, A.; Licursi, D.; Antonetti, C.; Valentini, G.; Galia, A.; o Di Nasso, N.N. Midinfrared FT-IR as a tool for monitoring herbaceous biomass composition and its conversion to furfural. *J. Spectrosc.* **2015**, *2015*, 719042. https://doi.org/10.1155/2015/719042.
18. Mwaikambo, L.Y.; Ansell, M.P. Chemical modification of hemp, sisal, jute, and kapok fibers by alkalization. *J. Appl. Polym. Sci.* **2002**, *84*, 2222–2234. https://doi.org/10.1002/app.10460.
19. Biswas, S.; Shahinur, S.; Hasan, M.; Ahsan, Q. Physical, Mechanical and thermal properties of jute and bamboo fiber reinforced unidirectional epoxy composites. *Procedia Eng.* **2015**, *105*, 933–939. https://doi.org/10.1016/j.proeng.2015.05.118.
20. Ray, D.; Sarkar, B.K.; Basak, R.K.; Rana, A.K. Study of the thermal behavior of alkali-treated jute fibers. *J. Appl. Polym. Sci.* **2002**, *85*, 2594–2599. https://doi.org/10.1002/app.10934.
21. Sinha, E.; Rout, S.K. Influence of fibre-surface treatment on structural, thermal and mechanical properties of jute fibre and its composite. *Bull. Mater. Sci.* **2009**, *32*, 65–76. https://doi.org/10.1007/s12034-009-0010-3.
22. Ray, D.; Sarkar, B.K.; Basak, R.K.; Rana, A.K. Thermal behavior of vinyl ester resin matrix composites reinforced with alkali-treated jute fibers. *J. Appl. Polym. Sci.* **2004**, *94*, 123–129. https://doi.org/10.1002/app.20754.
23. Suwan, T.; Maichin, P.; Fan, M.; Jitsangiam, P.; Tangchirapat, W.; Chindaprasirt, P. Influence of alkalinity on self-treatment process of natural fiber and properties of its geopolymeric composites. *Constr. Build. Mater.* **2022**, *316*, 125817. https://doi.org/10.1016/j.conbuildmat.2021.125817.
24. Shahinur, S.; Hasan, M.; Ahsan, Q.; Haider, J. Effect of chemical treatment on thermal properties of jute fiber used in polymer composites. *J. Compos. Sci.* **2020**, *4*, 132. https://doi.org/10.3390/jcs4030132.
25. Wang, H.; Memon, H.; Hassan, E.A.M.; Miah, S.; Ali, A. Effect of jute fiber modification on mechanical properties of jute fiber composite. *Materials* **2019**, *12*, 1226. https://doi.org/10.3390/ma12081226.
26. Rajesh, G.; Prasad, A.V.R. Tensile Properties of Successive Alkali Treated Short Jute Fiber Reinforced PLA Composites. *Procedia Mater. Sci.* **2014**, *5*, 2188–2196. https://doi.org/10.1016/j.mspro.2014.07.425.
27. Wang, Q.; Zhang, Y.; Liang, W.; Wang, J.; Chen, Y. Improved mechanical properties of the graphene oxide modified bamboo-fiber-reinforced polypropylene composites. *Polym. Compos.* **2020**, *41*, 3615–3626. https://doi.org/10.1002/pc.25648.
28. Sarker, F.; Potluri, P.; Afroj, S.; Koncherry, V.; Novoselov, K.S.; Karim, N. Ultrahigh Performance of Nanoengineered Graphene-Based Natural Jute Fiber Composites. *ACS Appl. Mater. Interfaces* **2019**, *11*, 21166–21176. https://doi.org/10.1021/acsami.9b04696.
29. Islam, M.H.; Afroj, S.; Karim, N. Toward Sustainable Composites: Graphene-Modified Jute Fiber Composites with Bio-Based Epoxy Resin. *Glob. Chall.* **2023**, *7*, 2300111. https://doi.org/10.1002/gch2.202300111.
30. Godara, S.S. Effect of chemical modification of fiber surface on natural fiber composites: A review. *Mater. Today Proc.* **2019**, *18*, 3428–3434. https://doi.org/10.1016/j.matpr.2019.07.270.
31. Singh, J.I.P.; Singh, S.; Dhawan, V. Effect of alkali treatment on mechanical properties of jute fiber-reinforced partially biodegradable green composites using epoxy resin matrix. *Polym. Polym. Compos.* **2020**, *28*, 388–397. https://doi.org/10.1177/0967391119880046.
32. Al-Oqla, F.M.; Sapuan, S.; Anwer, T.; Jawaid, M.; Hoque, M. Natural fiber reinforced conductive polymer composites as functional materials: A review. *Synth. Met.* **2015**, *206*, 42–54. https://doi.org/10.1016/j.synthmet.2015.04.014.
33. Mir, A.; Zitoune, R.; Collombet, F.; Bezzazi, B. Study of mechanical and thermomechanical properties of jute/epoxy composite laminate. *J. Reinf. Plast. Compos.* **2010**, *29*, 1669–1680. https://doi.org/10.1177/0731684409341672.
34. Doan, T.-T.; Brodowsky, H.; Mäder, E. Jute fibre/epoxy composites: Surface properties and interfacial adhesion. *Compos. Sci. Technol.* **2012**, *72*, 1160–1166. https://doi.org/10.1016/j.compscitech.2012.03.025.
35. Park, J.-M.; Kim, P.-G.; Jang, J.-H.; Wang, Z.; Hwang, B.-S.; DeVries, K.L. Interfacial evaluation and durability of modified Jute fibers/polypropylene (PP) composites using micromechanical test and acoustic emission. *Compos. Part B Eng.* **2008**, *39*, 1042–1061. https://doi.org/10.1016/j.compositesb.2007.11.004.

36. Rahman, M.; Mondol, M.; Hasan, M. Mechanical Properties of Chemically Treated Coir and Betel Nut Fiber Reinforced Hybrid Polypropylene Composites. *IOP Conf. Ser. Mater. Sci. Eng.* **2018**, *438*, 012025. https://doi.org/10.1088/1757-899x/438/1/012025.
37. Pa, P.; Sasikumar, M. Viscoelastic and mechanical behaviour of reduced graphene oxide and zirconium dioxide filled jute/epoxy composites at different temperature conditions. *Mater. Today Commun.* **2019**, *19*, 252–261. https://doi.org/10.1016/j.mtcomm.2019.02.005.
38. Sadangi, A.; Panda, K.K.; Kumari, K.; Srivatsava, M.; Dalai, N. Comparison study of various properties of jute reinforced composites with different nanofillers. *Mater. Today Proc.* **2021**, 16, 1239–1243. https://doi.org/10.1016/j.matpr.2021.06.332.
39. Alemour, B.; Badran, O.; Hassan, M.R. A Review of Using Conductive Composite. *J. Aerosp. Technol. Manag.* **2019**, *11*, e1919.
40. Yang, Q.-Q.; Gao, L.-F.; Zhu, Z.-Y.; Hu, C.-X.; Huang, Z.-P.; Liu, R.-T.; Wang, Q.; Gao, F.; Zhang, H.-L. Confinement effect of natural hollow fibers enhances flexible supercapacitor electrode performance. *Electrochim. Acta* **2018**, *260*, 204–211, https://doi.org/10.1016/j.electacta.2017.11.170.